Structure of the hepatitis C virus IRES bound to the human 80S ribosome: remodeling of the HCV IRES

5 AUTHORS, INCLUDING:

Rolf Thermann

GFE Blut mbH

18 PUBLICATIONS **1,170** CITATIONS

SEE PROFILE

Antje Ostareck-Lederer

University Hospital RWTH Aachen

39 PUBLICATIONS **2,440** CITATIONS

SEE PROFILE

Structure of the Hepatitis C Virus IRES Bound to the Human 80S Ribosome: Remodeling of the HCV IRES

Daniel Boehringer,[1,3,6] Rolf Thermann,[2,4,6,7]
Antje Ostareck-Lederer,[2,5,8] Joe D. Lewis,[2,7]
and Holger Stark[1,3,*]
[1]Max Planck Institute for Biophysical Chemistry
3D Electron Cryomicroscopy
Am Fassberg 11
37077 Göttingen
Germany
[2]Anadys Pharmaceuticals
3115 Merryfield Row
San Diego, California 92121

Summary

Initiation of translation of the hepatitis C virus (HCV) polyprotein is driven by an internal ribosome entry site (IRES) RNA that bypasses much of the eukaryotic translation initiation machinery. Here, single-particle electron cryomicroscopy has been used to study the mechanism of HCV IRES-mediated initiation. A HeLa in vitro translation system was used to assemble human IRES-80S ribosome complexes under near physiological conditions; these were stalled before elongation. Domain 2 of the HCV IRES is bound to the tRNA exit site, touching the L1 stalk of the 60S subunit, suggesting a mechanism for the removal of the HCV IRES in the progression to elongation. Domain 3 of the HCV IRES positions the initiation codon in the ribosomal mRNA binding cleft by binding helix 28 at the head of the 40S subunit. The comparison with the previously published binary 40S-HCV IRES complex reveals structural rearrangements in the two pseudoknot structures of the HCV IRES in translation initiation.

Introduction

The internal ribosome entry site (IRES) of hepatitis C virus (HCV) regulates viral protein expression by directly recruiting the ribosome to the start site of translation (Pestova et al., 2001). The single-plus-stranded RNA genome of HCV is 9600 nucleotides long and possesses a highly conserved IRES element in the 5′ untranslated region (5′ UTR) (Tsukiyama-Kohara et al., 1992; Wang et al., 1993). The IRES directs the ribosomal translation machinery directly to the start site of translation (Hershey and Merrick, 2000; Pestova et al., 2001); it constitutes a part—in the case of HCV, the major part—of

*Correspondence: hstark1@gwdg.de
[3]Lab address: http://www.mpibpc.mpg.de/groups/stark/
[4]Lab address: http://www-db.embl.de/jss/EmblGroupsHD/g_37.html
[5]Lab address: http://www.biochemtech.uni-halle.de/abiochemie/index.html
[6]These authors contributed equally to this work.
[7]Present address: European Molecular Biology Laboratory Heidelberg, Meyerhofstrasse 1, 69117 Heidelberg, Germany.
[8]Present address: Department of Biochemistry/Biotechnology, Martin Luther University Halle-Wittenberg, Kurt-Mothes-Str. 3, 06120 Halle/Saale, Germany.

the UTR. This is in contrast to canonical translation, in which the 5′-terminal cap of mRNA is recognized by translational initiation factors (eIF) and the 40S subunit, which scans the mRNA for the initiation codon at the start site of translation.

IRES-mediated translation of HCV RNA is initiated by the direct binding of a vacant 40S ribosomal subunit to the HCV IRES, a step that positions the initiation codon directly on the 40S subunit without scanning (Otto and Puglisi, 2004; Reynolds et al., 1996). This binary complex is joined by eIF3 and the ternary complex (Met-tRNA$_i^{MET}$/eIF2/GTP) to form a 48S complex that locks the initiation codon into the mRNA binding cleft of the 40S subunit (Ji et al., 2004; Pestova et al., 2001). In in vitro reconstitution experiments, the only initiation factors necessary for 48S complex formation are eIF2 and eIF3 (Pestova et al., 1998), but under the conditions of translation in vitro, further factors may be involved (Otto and Puglisi, 2004). The 48S complex is joined by the 60S subunit in a step mediated by eIF5b to form the 80S complex, and this leads to the formation of the first peptide bond (Pestova et al., 1998).

The secondary structure of the 5′ UTR in solution has been defined by phylogenetic comparison, biochemical probing, and mutational analysis (Brown et al., 1992; Wang et al., 1995; Zhao and Wimmer, 2001). The 5′ UTR can be divided into the 5′ part, which is mostly single-stranded and which includes the short stem loop of domain 1, and a 3′ part, which is highly structured and is essential for HCV IRES function (Pestova et al., 2001). The 3′ IRES part of the HCV UTR folds into three additional domains (for references, see above): (1) domain 2, a stem with several internal loops, (2) domain 3, a pseudoknot connected to a four-helix junction and stem loop 3d, and (3) domain 4, a small hairpin which includes the AUG start codon. The pseudoknot joins domain 2 with domain 3 and is also base paired to the sequence directly upstream of domain 4. The HCV IRES forms an extended structure that binds the 40S subunit by several synergetic interactions, and the domains involved in this binding have been determined by chemical and enzymatic footprinting experiments (Kieft et al., 2001; Kolupaeva et al., 2000). Mutational analysis has revealed the secondary structure elements essential for 40S binding and efficient translation (Honda et al., 1996; Otto and Puglisi, 2004; Pestova et al., 1998; Wang et al., 1995). The basal part of domain 3 (including principally the pseudoknot and stem loop 3d) includes the elements of secondary structure that determine the binding of the HCV IRES to the 40S subunit. In addition to providing affinity for the 40S subunit, the basal part of domain 3 may be required to position the initiation codon correctly in the decoding center of the 40S subunit, as indicated by "toeprinting" experiments (Otto and Puglisi, 2004; Pestova et al., 1998). The apical part of domain 3 binds eIF3 via stem loop 3b and the four-way junction (Buratti et al., 1998; Sizova et al., 1998). The binding of the HCV IRES to eIF3 is independent of the binding of the 40S subunit and is required for subunit joining, as has been shown by mutational analysis.

Domain 2 makes contact with the 40S subunit, but is not essential for subunit binding (Kieft et al., 2001). Deletion mutants of domain 2 have shown that this domain is required for subunit joining and mediates locking of the initiation codon onto the 40S subunit (Otto and Puglisi, 2004). Domain 4 forms a stem loop in solution, but is probably unwound in the IRES-40S complex (Honda et al., 1996). Several structures of HCV IRES fragments have been determined recently, either by nuclear magnetic resonance or by X-ray crystallography. However, these structures do not provide any information about tertiary interactions between the various fragments.

The structure of a reconstituted complex of the HCV IRES with the rabbit 40S subunit was determined by electron cryomicroscopy (cryo-EM) and allowed the localization of HCV IRES domains on the 40S subunit (Spahn et al., 2001b). The study showed that domain 3 is found on the solvent side of the 40S subunit body. The pseudoknot is positioned near the mRNA exit channel near the 40S platform, and domain 3b is located on the opposite side of the extended HCV IRES structure and protrudes into the solution. Domain 2 follows the intersubunit side of the 40S head and reaches into the tRNA exit side in the binary IRES-40S complex. Domain 2 mediates significant conformational changes in the 40S subunit when this subunit becomes bound to the HCV IRES; in particular, the pattern of contacts between head and body of the 40S subunit was found to be altered by the binding of HCV IRES. Recently, the structures of the cricket paralysis virus (CrPV) IRES in complex with the human 40S subunit and the human 80S ribosome were also determined by cryo-EM (Spahn et al., 2004). Although the mechanism of translation initiation differs significantly between HCV and CrPV, the IRES of these two viruses introduced similar conformational changes in the 40S subunit.

Progress has been made in the interpretation of the cryo-EM three-dimensional maps of eukaryotic ribosomes (Dube et al., 1998; Morgan et al., 2002; Spahn et al., 2001a). Because the conserved core of the ribosome is shared between organisms ranging from bacteria to mammals, the atomic resolution crystal structures of the bacterial ribosomal subunits could be fitted into the electron microscopic maps of eukaryotic ribosomes; this allowed a homology-based model of the yeast ribosome to be built (Spahn et al., 2001a).

Here, we present the structure of the HCV IRES in complex with the human 80S ribosome, determined by electron cryomicroscopy. The IRES-80S complex was prepared under in vitro translation conditions and was stalled by cycloheximide directly before elongation. To our knowledge, this is the first IRES-ribosome structure obtained under near native conditions. Docking HCV IRES fragments with known X-ray or NMR structures allowed a detailed structural interpretation of the HCV IRES-80S ribosome interactions. The structure reveals a complex network of interactions between the HCV IRES and the 40S subunit, but only a single point of contact between the HCV IRES and the 60S subunit. We propose a model for the coupled conformational rearrangement of the HCV IRES mediated by initiation factor binding.

Results

Tobramycin Affinity Purification of the HCV IRES Complex with the 80S Ribosome

The tobramycin affinity purification method (Hartmuth et al., 2002) was adapted for the isolation of human 80S translation complexes under native conditions. A HeLa cell-derived in vitro translation system (Bergamini et al., 2000) was used to assemble native 80S translation-competent complexes on the HCV IRES under conditions that allow efficient translation. For the purification of 80S translation complexes, cycloheximide was added to the translation reactions in order to stall the translation process at the initiation stage.

An RNA aptamer of length 40 nt was inserted into a 5′ UTR derived from a hepatitis C genomic sequence, the genotype 1b (Ostareck-Lederer et al., 2005). This aptamer binds with high affinity (5 nM) to the aminoglycoside antibiotic tobramycin under physiological conditions (Hamasaki et al., 1998). The presence of the aptamer in the HCV IRES does not interfere with the formation of translation-competent 80S complexes and does not significantly affect the translation of a firefly luciferase reporter RNA fused to the aptamer-containing the HCV IRES (data not shown).

To test the purity and integrity of the isolated 80S complexes, an aliquot of the isolate was reloaded on a linear 5%–25% sucrose gradient (Figure 1A). The majority of the ribosomal complexes sedimented in a single peak in the 80S region and only small amounts of 48S translational initiation complexes and smaller RNPs were detected. Additionally, an aliquot of the isolate was analyzed by 7.5%–15% SDS PAGE and proteins were detected by silver staining (Figure 1B). The specificity of the isolation is shown in Figure 1B, where a strong enrichment of bands corresponding to the purification using the aptamer-tagged RNA (Figure 1B, Tob-IRES) can be seen when compared with the purification using an untagged HCV-5′ UTR (Figure 1B, IRES).

The HCV IRES Induces Conformational Changes in the 80S Ribosome

The structure of the HCV IRES in complex with the 80S ribosome, referred to as the IRES-80S complex, was reconstructed at 15 Å resolution (as judged by Fourier shell correlation using the 3 σ criterion; 25 Å using the 0.5 criterion; see Figure S1 in the Supplemental Data available with this article online). Ribosomes share a high degree of sequence and structural conservation across all kingdoms (Dube et al., 1998; Morgan et al., 2002; Spahn et al., 2001a). Crystal structures of bacterial ribosomes were recently used to build a homology-based atomic model of the conserved RNA sequences and proteins in the 3D density maps of the *Saccharomyces cerevisiae* ribosome (Spahn et al., 2001a) and canine ribosomes (Morgan et al., 2002). These models allow a detailed interpretation of the IRES-80S complex structure.

The structure of the 80S ribosome in complex with the HCV IRES is significantly different from the structure of elongating 80S ribosomes (Figure 2). Elongating 80S ribosomes were stalled on cellular mRNA under in vitro translation conditions by blocking translocation with cycloheximide. The structure of the elongating 80S ribosome was reconstructed (resolution 28 Å) and aligned

A

B
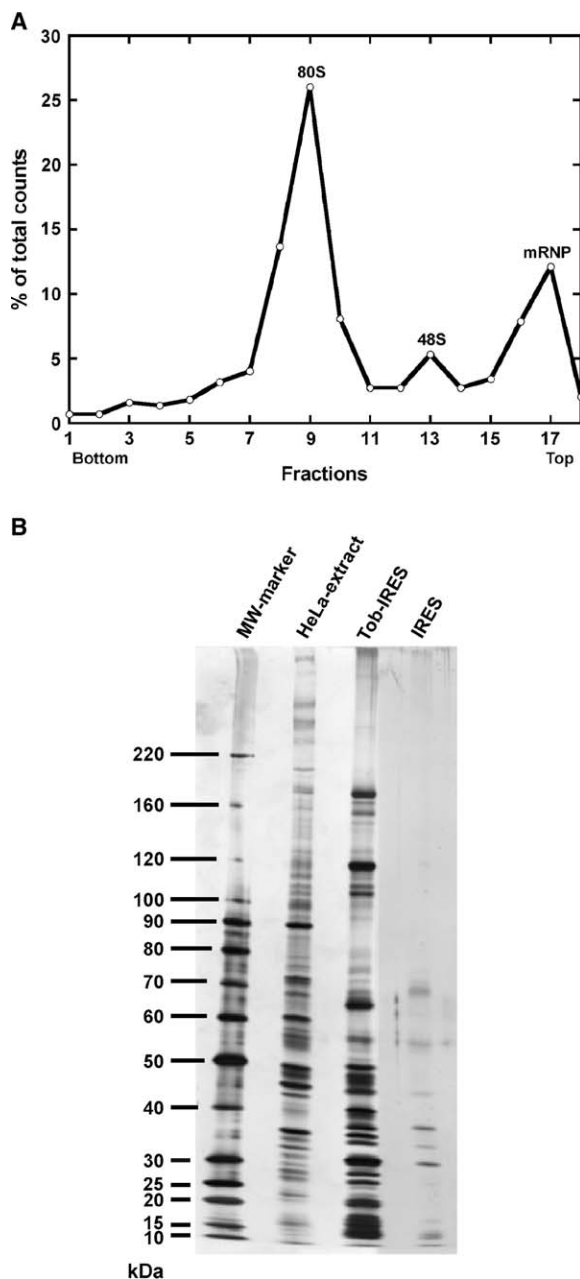
Figure 1. Purification of Native Ribosomal IRES-80S Complexes by Tobramycin Affinity Selection and Sucrose Gradient Centrifugation

(A) The 80S ribosomal complexes were purified from sucrose gradient fractions by the tobramycin affinity purification method; they were then reloaded onto a 5%–25% sucrose gradient for analysis.

(B) SDS-PAGE analysis of the proteins isolated from the 80S gradient fractions. Proteins from gradient fractions were precipitated and loaded onto a 7.5%–15% gradient SDS polyacrylamide gel. Protein bands were visualized by silver staining. MW-marker, molecular weight marker; HeLa extract, 3 μg of crude HeLa extract; Tob-IRES, eluate of the 80S gradient fraction using the Tob-tagged HCV IRES (as used for EM studies); IRES, eluate of the 80S gradient fraction using an untagged HCV IRES.

to the 80S ribosome in complex with the HCV IRES. The difference map between the two structures allows the density of the HCV IRES to be separated from that of the ribosomal subunit. The HCV IRES is in contact with

the 40S subunit at the back of the head and the body and at the solvent side close to the tRNA exit site (Figure 2B). The only interaction found between the HCV IRES and the 60S subunit was with the L1 protuberance (Figures 2C). The expansion segments of the 60S subunit display minor differences between the IRES-80S complex and the elongating ribosome. The most distinct change occurs in ES 27 (Figure S2), but is probably unrelated to IRES binding, as the conformation of expansion segment 27 differs significantly depending on the N-terminal sequence of the nascent peptide chain (Beckmann et al., 2001). The back of the 60S subunit is covered by a group of density elements that can be attributed to ES 7, ES 11, and ES 15 (Figure 2A). The mass observed for ES 7 and ES 27 represents only a small fraction of the density expected for the entire RNA expansion segment. This is probably due to the flexibility of these RNA elements.

The atomic homology model of the yeast ribosome can be used to obtain a molecular model of the 80S ribosome and allows the assignment of structural domains to individual RNA helices and ribosomal proteins (Spahn et al., 2001a) (Figure 3A). The yeast homology model fits well into the body and head back, but the fit is less accurate at head beak. The conformation of the head beak is different in the IRES-80S complex and the elongating 80S ribosome. The head beak is bent toward the intersubunit space in the IRES-80S complex, compared with the elongating 80S ribosome. The rearrangement of the head beak involves helices 32 and 33 and protein S3 (Figure 3B). In the structures of the IRES-80S complex and the elongating ribosome, the mRNA entry channel at the head beak is locked by an interaction of helix 18 on the head with helix 34 on the body of the 40S subunit (Figure 3B). In the IRES-80S complex, an additional contact occurs at the solvent side of the 40S subunit between helix 16 of the body and protein S3 on the head (Figure 3B). The mRNA exit channel at the head back is closed by a connection of 40S subunit protein S5 and S14. Thus, the closure of the mRNA exit and entry channels is accompanied by conformational changes in the head beak of the IRES-80S complex.

The density of the head lobe is smaller in the IRES-80S complex than in the elongating 80S ribosome (Figures 2A and 2B). The head lobe was recently assigned to RACK1 (Sengupta et al., 2004). The smaller head lobe density observed in the IRES-80S complex structure is due to a reduced occupancy of RACK1. This can be shown by computationally separating the image data set in complexes bearing RACK1 and complexes devoid of RACK1. We found 52% occupancy of RACK1 in the IRES-80S complex (data not shown).

Structure of the HCV IRES

The HCV IRES density (Figure 4) consists of a rod-shaped upper domain that is in close contact with the head. The apical part of this domain is bent so that it points into the tRNA exit site. In a recent EM study of binary HCV IRES-40 complexes (Spahn et al., 2001b), this density was found to be missing after the deletion of domain 2. Consequently, this part of the HCV IRES density can be assigned to domain 2, and the remaining density can be attributed to domains 1 and 3. The density of domains 1 and 3 may be subdivided into five
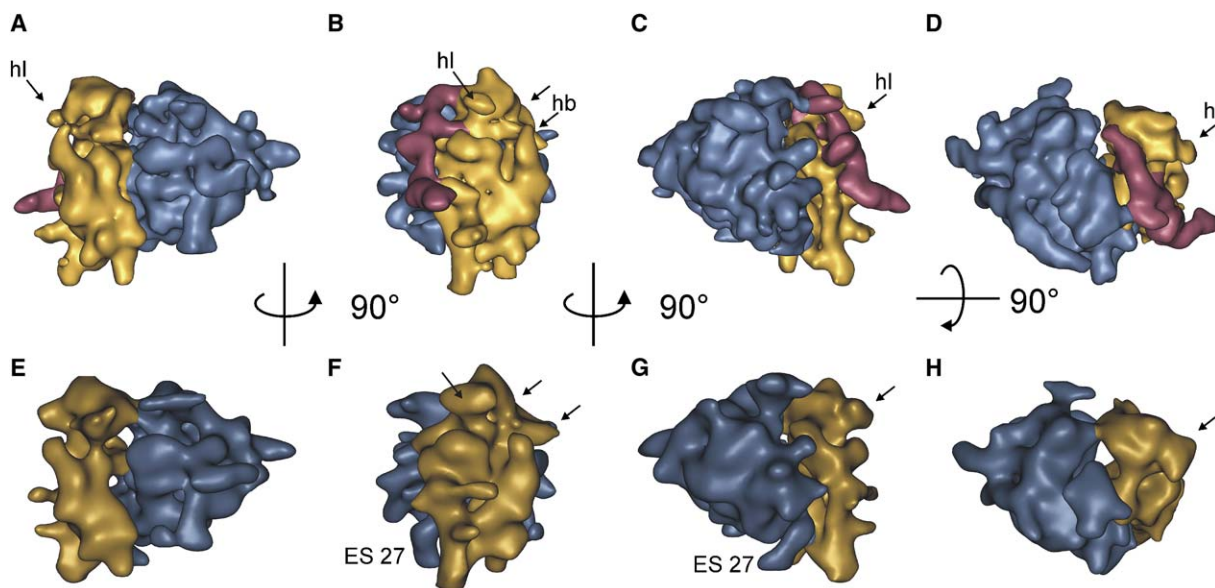
Figure 2. The Three-Dimensional Structure of the Cycloheximide-Stalled IRES-80S Complex and, for Comparison, an Elongating 80S Ribosome Stalled by Cycloheximide

(A–D) Cycloheximide-stalled IRES-80S complex; (E–H) elongating 80S ribosome stalled by cycloheximide. (A)–(C) and (E)–(G) give a lateral view, (D) and (H) a tilted view. The difference density between the two structures reveals additional density on the IRES-80S complex that can be attributed to the HCV IRES (purple). The 40S subunit is shown in gold, the 60S subunit in blue. The HCV IRES density is mainly in contact with the 40S ribosomal subunit. Arrows indicate the major differences between the IRES-80S complex and the elongating 80S ribosome in the head lobe (hl), the head beak (hb), and the 28S rRNA expansion segment (ES 27).

density elements, as follows. An L-shaped region of density (Figure 4, I) is located at the proposed exit path of the mRNA at the base of the head, which is connected to a small protrusion (p) at the junction to domain 2. The remaining density follows the back of the 40S subunit from the head downward. It forms a density lobe (o) connected to another globular domain (g). A rod-shaped extension (e) of the globular domain protrudes into solution.

Several recently published structures of HCV IRES domains determined by NMR (Collier et al., 2002; Klinck et al., 2000; Lukavsky et al., 2000, 2003) and X-ray crystallography (Kieft et al., 2002) were placed in the HCV IRES density (Figure 5). The entire length of the HCV IRES density can only be spanned by an extended structure of the HCV IRES. Furthermore, the diameter of the rod-shaped density elements is similar to the diameter of a single A-RNA helix, suggesting that the HCV IRES RNA mainly adopts an extended helical conformation. The HCV IRES density that follows the intersubunit side of the 40S head can be fitted with the NMR structure of full-length domain 2. The extended density on top of the 40S head and the missing density in the region of the terminal loop may be attributed to rearrangements of the 40S head in the IRES-80S complex compared with the elongating 80S ribosome. The small protrusion (p) at the stem base of domain 2 pointing into solution is attributed to domain 1. This protrusion is missing in the binary IRES-40S structure that used an HCV IRES construct lacking domain 1 (Spahn et al., 2001b) (Figure S3). However, there is not enough density to accommodate the entire length of domain 1. The sequence between the pseudoknot and domain 1 is predicted to be

single-stranded and thus to possess considerable flexibility. It is therefore unlikely that the entire density of this domain will be visible in the reconstruction.

According to the connectivity of the secondary structure model, domain 3b is expected to form the opposite end of an elongated HCV IRES structure. The rod-shaped extension (e) protruding into solution can thus be assigned to domain 3b and the corresponding NMR structure (Collier et al., 2002) of the internal loop fits precisely into this density. The terminal loop of domain 3b, which is not included in the NMR structure, may fill in the remaining density at the apex of the protrusion.

Domain 3b is connected to the four-way junction including stem loop 3a/c. The globular density (g) connected to domain 3b can thus be assigned to the four-way junction. The four-way junction consists of four arms: stem loops 3a and 3c, the base of domain 3b, and the fourth arm that connects the four-way junction to the basal part of domain 3, referred to as arm 3*. The four-way junction was recently crystallized as a dimer (Kieft et al., 2002), and the monomer can be placed in the globular density. However, the fit is not very accurate in the loop regions of the stem loops 3a and 3c. Furthermore, the helical stacking in the four-way junction entails a parallel arrangement of stem 3b and arm 3*. This in turn requires the connection of arm 3* to domain 3b to be kinked, which is difficult to bring in line with the proposed secondary structure model of the HCV IRES. A recent fluorescence resonance energy transfer study of the global conformation of the isolated four-way junction suggested an equilibrium between a parallel and an antiparallel orientation of coaxial stacked helices (Melcher et al., 2003). Therefore, the four-way junction
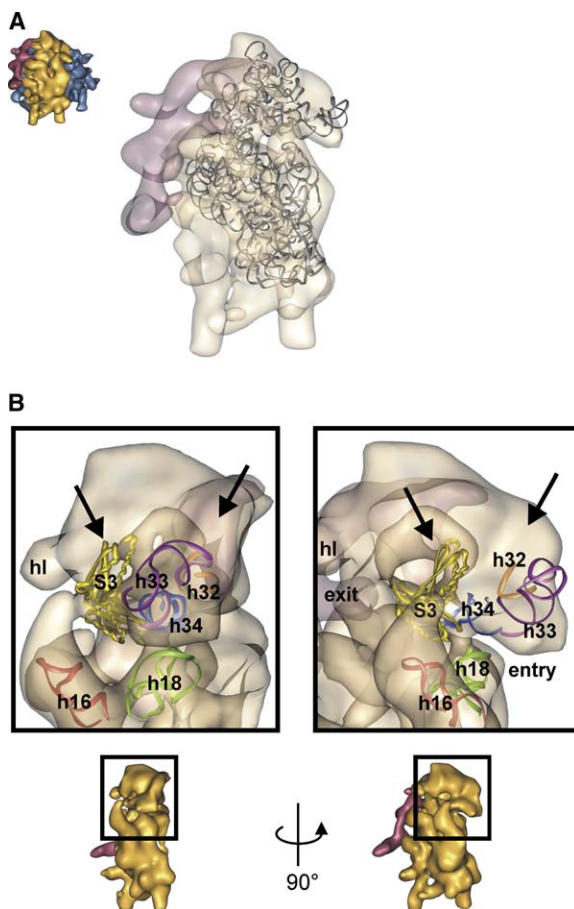
Figure 3. The mRNA Entry and Exit Channel of the 40S Subunit in the IRES-80S Complex

(A) The atomic model for the evolutionarily conserved core of the yeast 80S ribosome (Spahn et al., 2001a) was placed in a 3D density map of the 40S ribosomal subunit that had been computationally cut out of the IRES-80S complex.

(B) The entry channel is closed by a connection of helix 18 (green) with helix 34 (blue). On the solvent side, helix 16 (red) is in contact with the head, while protein S3 (yellow, homologous with prokaryotic S3) is connected to helix 34. "hl" denotes the head lobe that does not show any connection with the body. The conformation of the head is considerably different in the IRES-80S complex from that in the elongating 80S ribosome, as indicated by the two pairs of arrows, which point out helices 32 (orange) and 33 (magenta).

may adopt an antiparallel conformation on the 40S subunit. This conformation would not require the kinked structure of arm 3*.

Stem loop 3d is connected, by a short base-paired region, to the four-way junction. Thus, the lower part of the lobe-shaped domain (o) is assigned to domain 3d. The remaining lobe-shaped density is attributed to the connection between domain 3d and the pseudoknot. The fit of the NMR structure of domain 3d (Klinck et al., 2000; Lukavsky et al., 2000) represents only one of several possible orientations, as the resolution of the IRES-80S structure is not high enough to separate individual RNA strands of complex secondary structure elements. The L-shaped appearance of the density located at the mRNA exit channel is reminiscent of a tRNA and might harbor the cloverleaf structure of the pseudoknot. This is consistent with the results of RNase P cleavage stud-

ies that indicate the existence of a tRNA-like shaped structure near the initiation codon (Lyons et al., 2001). The only atomic structure obtained so far for the pseudoknot is the small stem loop 3e. This structure could not be fitted in unambiguously, because individual RNA strands are not resolved. In order to place the initiation codon in the decoding site, domain 4 is probably unwound (Honda et al., 1996). As stated above, single-stranded RNA is not seen at the present level of resolution, so this domain is not included in the difference density.

HCV IRES Contacts on the Ribosome

The atomic homology model of the yeast ribosome (Spahn et al., 2001a) allows the assignment of contact points of the HCV IRES on individual helices and proteins of the ribosome. The HCV IRES contacts the ribosome on the 60S subunit at the L1 stalk (Figure 4D) and at four different sites on the 40S subunit (Figure 4A). Domain 2 interacts with protein S5 on the intersubunit side of the 40S head (Figure 6A). Protein S5 forms the mRNA exit channel together with protein S14 (Spahn et al., 2001a). The apex of domain 2 reaches into the tRNA exit site close to the loop regions of helices 23 and 24 of the 40S subunit (Figure 6A). Domain 3 contacts the ribosome at three different sites that join the 40S head to the back lobes of the 40S subunit body. The pseudoknot interacts with the back of the 40S head at helices 28, 37, and 40, but bypasses protein S14 and the shoulder of the 40S subunit (Figure 6B). The pseudoknot at the head is connected to domain 3d, which forms the most extensive contact of the HCV IRES on the 40S subunit body. This interaction probably involves ES 7, the extension of helix 26. The contact could be mediated by direct RNA-RNA interactions, as it is also observed at higher density thresholds. RNA remains visible at higher thresholds owing to the higher scattering intensity of nucleic acids compared to proteins. Furthermore, the 40S subunit lacks the proteins that reside in the vicinity of helix 26 on the bacterial 30S subunit surface; it may thus display RNA on the surfaces in this region (Spahn et al., 2001a). Domain 3b is connected to the four-way junction that forms the second contact of the HCV IRES on the 40S subunit body. One side of the four-way junction interacts with the 40S subunit near ES 6 (Figure 6C). This interaction area is less extensive than the contacts made by domain 3d with the body and the pseudoknot at the head. The lack of reliable data on the location of 40S subunit proteins, which are not homologous with those of the bacterial 30S subunit, prohibits the identification of the proteins involved in this interaction.

Discussion

Conformation of the Human 80S Ribosome in Complex with the HCV IRES

To understand HCV IRES function, it is essential to study IRES-mediated initiation of translation under conditions as close as possible to those in vivo. Here, we present the 3D structure of the HCV IRES in complex with the human ribosome, formed under translation conditions, as determined by electron cryomicroscopy. The tertiary structure of the HCV IRES is of major importance for IRES function, as single base substitutions can severely reduce translation efficiency, and because several
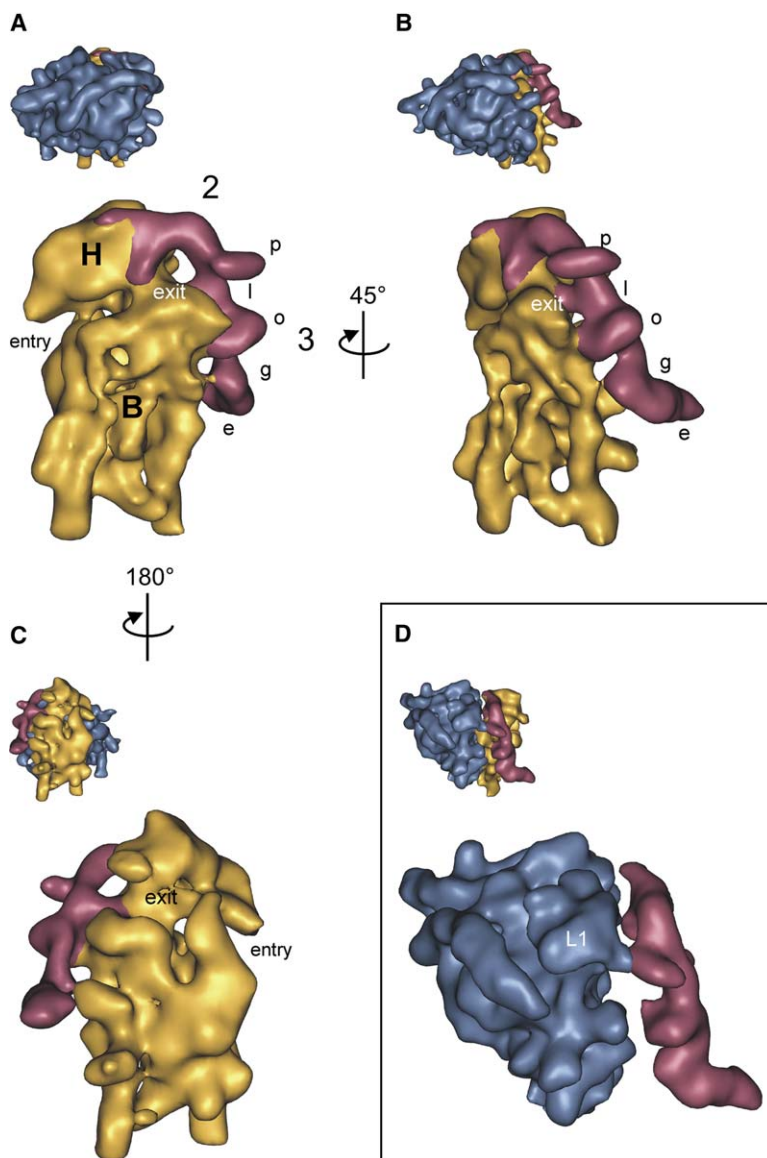
Figure 4. Surface Representation of the 40S Ribosomal Subunit (Yellow) and 60S Ribosomal Subunit (Blue) in Complex with the HCV IRES (Purple) in the IRES-80S Complex

(A–C) The 60S subunit is omitted for improved visualization of the HCV IRES structure (top, IRES-80S complex in the corresponding orientation) as seen from the intersubunit side (A), the mRNA exit channel side (B), and the solvent side (C). The mRNA exit and entry channels are labeled. H and B indicate the head and the body. The HCV IRES densities are assigned as follows: 2, domain 2; 3, domain 3. Domain 3 comprises five density elements: L-shaped density, l; lobe-shaped density, o; protrusion, p; globular density, g; extension, e.

(D) The 40S subunit is omitted. The HCV IRES makes contact with the 60S ribosomal subunit at the L1 stalk labeled L1.

domains act cooperatively in positioning the initiation codon on the ribosome. The IRES-80S complexes had been stalled by cycloheximide after subunit joining and before translocation. The IRES is still bound in the ribosomal E site, confirming an efficient block of translocation (see below). The IRES-80S structure presented here thus represents a well-defined HCV IRES complex in the final stage of initiation of translation.

The conformation of the 60S subunit in the IRES-80S complex is very similar to the 60S subunit in the elongating 80S ribosome and to the recently published structure of the posttranslational 80S ribosome (Spahn et al., 2004). The only differences observed occur in areas of known structural heterogeneity. The conformation of ES 27 is different in the elongating 80S ribosome but is probably unrelated to HCV IRES binding, as the conformation of expansion segment 27 differs significantly depending on the N-terminal sequence of the nascent peptide chain (Beckmann et al., 2001). In all structures of mammalian ribosomes, the densities corresponding to the expansion segments ES 7 and ES 27 are not com-

pletely visible, probably because of flexibility in these large RNA elements (Dube et al., 1998; Morgan et al., 2002; Spahn et al., 2004) (Figure S2). These relatively large flexible parts in the structure of mammalian ribosomes compared to bacterial, fungal, and plant ribosomes may also be an important resolution-limiting factor.

The HCV IRES induced significant conformational changes in the structure of the 40S subunit in the IRES-80S complex. In a recent paper, the structure of a binary IRES-40S complex was presented (Spahn et al., 2001b). Functionally, this complex probably represents the initial stage of complex formation between the HCV IRES and the 40S subunit as observed in in vitro translation systems (Otto and Puglisi, 2004). The IRES-80S complex represents the final stage of translation initiation. The comparison of these two structures allows one to follow the conformational changes during HCV translation initiation. In the free 40S subunit, the mRNA entry channel is closed. On HCV IRES binding, the entry channel is opened in the IRES-40S complex, probably to
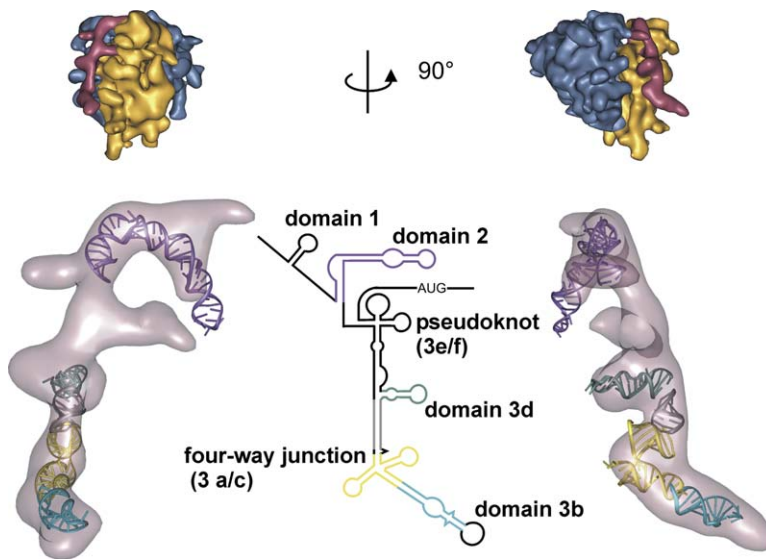
Figure 5. Fitting of the Known NMR and Crystal Structures to the HCV IRES Density

Above is the complete IRES-80S complex; below, the HCV IRES in the same orientation. The numbering of the domains follows their order in the RNA sequence (center). Domain 2 in the upper end of the HCV IRES density is shown in magenta. Domain 3d is shown in green below the pseudoknot (which includes domains 3e and 3f). The four-way junction including domains 3a and 3c is colored yellow. The base-paired sequence connecting domain 3d to the four-way junction is represented by an A RNA helix (gray). Domain 3b in the lower end of the HCV IRES density is shown in cyan. Domain 4 (not labeled) is the 3′-terminal end including the AUG codon; this domain is not visualized in the HCV IRES density (see text). The secondary structure of the HCV IRES (center) is depicted in an orientation reflecting the architecture of the HCV IRES with the domains color coded as above. Sufficient space remains in the IRES density map for the regions for which no high-resolution structure information is available (black in the schematic representation).

allow the downstream sequence of the HCV RNA to bind. It is closed again as translation initiation proceeds, as observed in the IRES-80S complex. Whereas the conformation of the mRNA entry channel is highly variable, the mRNA exit channel (proteins S5 and S14 and helix 28) is closed in the binary IRES-40S (Spahn et al., 2001b) and IRES-80S complexes.

In the IRES-80S complex, the HCV IRES may induce a conformational change of the mRNA entry channel (helix 18 in the body, and helix 34 in the head) by altering the conformation of the head beak (involving helices 32 and 33). The tip of the head beak, helix 33, points toward the intersubunit space. This conformational rearrangement could stabilize the closure of the entry channel by helix 18 and helix 34. A movement of the head beak was suggested to occur upon binding of the HCV IRES to the 40S subunit (Spahn et al., 2001b). This results in contact between protein S3 on the head and helix 16 of the body. The contact of protein S3 with helix 16 could also be observed for the IRES-80S complex. Tentatively, this contact might stabilize the relative orientation of head and body during the structural rearrangements at the mRNA entry channel. The conformational changes at the mRNA entry channel might alter accessibility of the viral open reading frame RNA and could cause the altered pattern of toeprints after eIF2-mediated 48S complex formation (Pestova et al., 1998). This may suggest that the conformational rearrangements of the head beak occur upon codon recognition in the 48S complex.

In addition to the conformational changes at the mRNA binding cleft, the occupancy of RACK1 was significantly reduced in the IRES-80S complex. The HCV IRES together with cellular factors present in cell extract may dissociate RACK1. RACK1 was implicated in eIF4E phosphorylation by recruiting activated protein kinase C to the ribosome (Nilsson et al., 2004). Tentatively, the dissociation of RACK1 may result in a dephosphorylation of eIF4E and may thus repress cap-mediated translation and assist IRES-mediated translation (Scheper and Proud, 2002).

Interactions of the HCV IRES Domain 2 with the Ribosome

The large structural rearrangements of the 40S subunit head and beak might be facilitated by domain 2, as they are absent in the structure of an HCV IRES domain 2 deletion bound to the 40S ribosome (Spahn et al., 2001b). Deletion of domain 2 permitted formation of the 48S complex, but abolished formation of the 80S complex, in in vitro translation systems (Ji et al., 2004; Otto and Puglisi, 2004). Thus, the conformational change of the head induced by domain 2 may be required not only to stabilize the proper positioning of the initiation codon, but also for joining the subunits. Domain 2 may mediate the positioning of the initiation codon in the ribosomal P site by direct interactions with the E site-bound domain 4 or through interactions with protein S5 (Fukushi et al., 2001) and helices 23 and 24. In line with these results, toeprinting assays of domain 2 deletion mutants indicated a less stable binding of the initiation codon by the 40S subunit (Otto and Puglisi, 2004; Pestova et al., 1998). However, domain 2 is not sufficient to position the initiation codon on the ribosome (Otto and Puglisi, 2004). Domain 2 folds independently of domain 3 in solution and is probably flexibly linked to domain 3 (Beales et al., 2001; Lukavsky et al., 2003).

In the progression to elongation, domain 2 has to be moved out of the ribosomal E site to make space for deacylated tRNA. Because domain 2 occupies the E site, it has to be removed before—or during—the first elongation event to allow normal tRNA binding (Morgan et al., 2002; Spahn et al., 2001b). The role of the L1 stalk could be analogous to the function of the stalk in bacterial translation. Studies of *Escherichia coli* ribosomes stalled before and after elongation suggested that the L1 stalk might be involved in the removal of E site-bound tRNA (Valle et al., 2003). Cycloheximide is bound near the E site and may hinder the removal of domain 2 in addition to blocking translocation (Pestova and Hellen, 2003). This may explain why HCV IRES-80S complexes
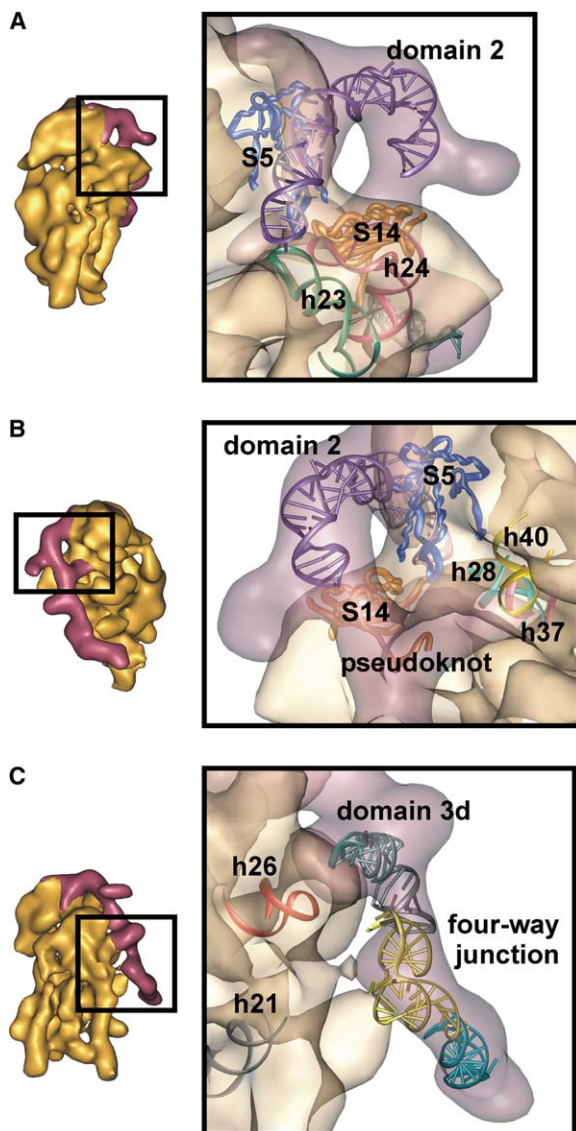
Figure 6. Contact Sites of the HCV IRES on the 40S Ribosomal Subunit

(A) Contacts of the HCV IRES (transparent purple) on the 40S ribosomal subunit (transparent yellow). The contact site of HCV IRES domain 2 (magenta) is partially occupied by ribosomal protein S5 (blue), homologous with prokaryotic S7. Protein S5 closes the mRNA exit channel by making contact with protein S14 (homologous with prokaryotic S11).
(B) Contacts between the basal pseudoknot of domain 3 on the 40S subunit involving helix 28 (cyan), helix 37 (red), and helix 40 (yellow) of 18S rRNA.
(C) The contact site of domain 3d (green) is located near helix 26 of 18S rRNA (red). In the eukaryotic 40S subunit, helix 26 is extended to expansion segment 7. The four-way junction (yellow) contacts the 40S subunit at ES 6, located below helix 21. Domain 3d (cyan) protrudes into solution.

are more sensitive toward cycloheximide than canonical 80S initiation complexes are (Dmitriev et al., 2003; Pestova and Hellen, 2003). Cycloheximide has been used recently to stabilize nascent chain complexes in yeast (Beckmann et al., 2001). In these complexes, a P site-bound tRNA was detectable, which is not the case in the IRES-80S complex. However, the tRNA may dis-

sociate if the nascent chain is missing, as has been described for puromycin-treated samples of ribosome-translocon complexes (Morgan et al., 2002). We cannot exclude that the IRES-80S complex undergoes minor structural rearrangements upon dissociation of the P site tRNA. However, these effects are probably small, as for example ribosome-translocon complexes with and without P site tRNA, obtained by different purification protocols, were structurally very similar (Beckmann et al., 2001; Menetret et al., 2000; Morgan et al., 2002).

Conformational Changes in HCV IRES Domain 3 upon 80S Complex Formation

The overall appearance of the HCV IRES density is similar in the binary IRES-40S and the IRES-80S complex structures (Spahn et al., 2001b) (Figure S3). The major features of the HCV IRES density—namely, domain 2 in close contact with the head and the three globular domains on the back of the 40S particle connected to an elongated domain—can be identified in both structures. The mRNA protection patterns of the IRES-48S and IRES-80S complexes are unchanged, suggesting that the conformation of the HCV IRES is similar in these two complexes (Lytle et al., 2001). However, local conformational changes of the HCV IRES are observed for the pseudoknot and the four-way junction in the IRES-80S complex compared with the IRES-40S complex. These structural elements may be involved in active transformation of the IRES-40S complex to the IRES-80S complex mediated by eIF2 and eIF3.

In the IRES-80S complex, the pseudoknot was assigned to the triangular domain located at the mRNA exit channel at helix 28 and protein S5. There is no contact of the platform region of the 40S subunit with the HCV IRES in the IRES-80S complex. In contrast, the binary IRES-40S shows a broad contact interface of the pseudoknot sequence with the platform. Thus, the conformation of the pseudoknot at the mRNA exit path changes in the transition from the IRES-40S to the IRES-80S complex. In line with these findings, toeprinting experiments indicated that conformational changes may be necessary for the proper positioning of the initiation codon in the ribosomal P site (Otto and Puglisi, 2004; Pestova et al., 1998).

Helix 28 lines the exit site of the mRNA, as shown in a crystallographic study of the bacterial ribosome (Yusupova et al., 2001). This suggests that the single-stranded domain 4 enters the mRNA exit channel of the eukaryotic ribosome at the same site as the bacterial mRNA bound to the 3′ end of the 18S rRNA does. The visualized density at the mRNA exit path may thus include stem loop 3f, which binds the single-stranded sequence connecting the pseudoknot and the unwound domain 4. Mutations in domain 3f reduced the translation efficiency significantly without affecting affinity for the 40S subunit, suggesting a functional requirement for this domain in positioning the initiation codon (Kieft et al., 2001; Wang et al., 1995).

The stem loop 3d makes the most extensive contacts with the 40S subunit body in the IRES-80S complex and the binary IRES-40S complex. This contact may be mediated by RNA-RNA interactions with ES 7 and provide a stable anchor point of the HCV IRES on the back of the 40S subunit body. Domain 3d is found to be
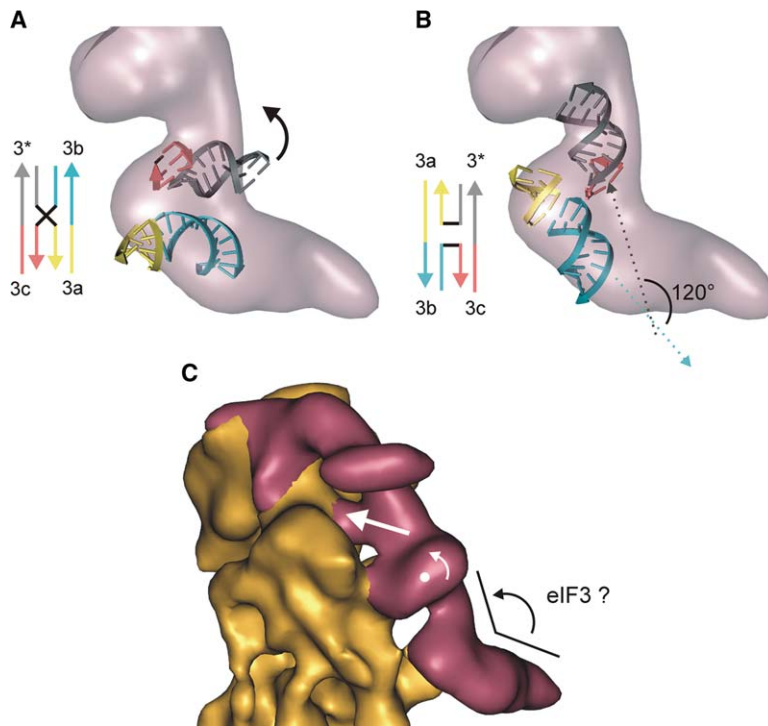
Figure 7. Conformation of the Four-Way Junction

The parallel conformation of the four-way junction in the crystal structure is compared with an antiparallel model of the global junction conformation as suggested by fluorescence resonance energy transfer measurements. The base-paired sequences of the arms of the four-way junction are represented by A form helices. Arm 3* (gray) stacks on stem 3c (red), and stem 3b (blue) stacks on stem 3a (yellow).
(A) In the crystal structure, the four-way junction arms 3* and 3b are in a parallel orientation, and arm 3* needs to be kinked to fit the density (indicated by a solid arrow).
(B) In the model of the antiparallel conformation of the four-way junction, the angle between arms 3* and 3b is 120° (indicated by gray and blue dotted arrows) and arm 3* fits the density without further adjustments.
(C) Model for the coupled conformational change of IRES domain 3. A conformational rearrangement of the four-way junction (black arrow) could be transmitted by a lever-like movement to the basal pseudoknot (white arrows). Domain 3d could be the pivot point of the lever movement exerted by eIF3 binding to the four-way junction.

protected by the addition of the 40S subunit (Kieft et al., 2001; Kolupaeva et al., 2000) and certain mutations in the loop and internal bulge can abolish HCV IRES binding (Ji et al., 2004; Jubin et al., 2000; Odreman-Macchioli et al., 2001; Otto and Puglisi, 2004).

The density bridge connecting domain 3d on the back of the 40S subunit with the pseudoknot on the 40S head is well defined, and it may restrain the position of the initiation codon relative to the mRNA binding cleft. Consistently with a tight coupling between domain 3d and the pseudoknot, a point mutation in the helix between domain 3d and the pseudoknot was found to compromise the positioning of the initiation codon on the 40S subunit (Otto and Puglisi, 2004). The mutation did not affect 40S binding affinity significantly; however, the translation efficiency was significantly reduced. Furthermore, the toeprint pattern changed, so as to resemble the pattern of the binary IRES-40S complex (Otto and Puglisi, 2004). In addition to providing binding affinity, domain 3d may therefore function as an anchor point for the proper positioning of the pseudoknot at the head.

The second contact of the HCV IRES on the body of the 40S subunit in addition to domain 3d is located at the four-way junction. The four-way junction makes contact with the 40S subunit body at ES 6 in the IRES-80S complex and the binary IRES-40S complex. The four-way junction forms the connection to domain 3b, which has been shown to bind eIF3 independently of interactions with the 40S ribosomal subunit (Ji et al., 2004; Kieft et al., 2001; Sizova et al., 1998). The crystal structure presented in Figure 5 represents the parallel orientation of the coaxial stacked helices, whereas the antiparallel orientation may also exist in solution (Melcher et al., 2003). The parallel orientation of arm 3* and stem 3b in the crystal structure would require arm 3* to be kinked by more than 90° (Figure 7A). However, a kinked struc-

ture of arm 3* is not supported by the secondary structure analysis. A model of the antiparallel coaxially stacked helices provides a better fit for the density of the four-way junction in the IRES-80S complex and does not require arm 3* to be kinked (Figure 7B). The angle between the coaxially stacked helices 3*/3a and 3c/3b in the model is 120°, as observed for antiparallel conformations of nucleic acid junctions (Lilley, 2000). In the IRES-40S complex, the angle between the arms 3* and 3b appears to be smaller (Spahn et al., 2001b) (Figure S3). This suggests a shift from the parallel conformation of the four-way junction to the antiparallel conformation in the progression from the IRES-40S to the IRES-80S complex.

The four-way junction is functionally important for HCV IRES activity. Introduction of point substitution mutations greatly reduced the efficiency of translation (Rijnbrand et al., 2004), while deletion mutations abolished the formation of the 48S complex (Otto and Puglisi, 2004). Furthermore, the toeprint pattern of a domain a/b/c deletion mutant resembled the toeprint pattern of the binary IRES-40S complexes (Otto and Puglisi, 2004). This indicates that the mutant bearing a deletion in the four-way junction fails to position the basal pseudoknot and the initiation codon correctly. This suggests, in turn, that the four-way junction is the second element on the body mechanistically coupled to the pseudoknot, in addition to domain 3d. The binding of eIF3 is required for subunit joining (Pestova et al., 1998), thus tentatively eIF3 could alter the conformation of the HCV IRES by stabilizing the antiparallel orientation of the four-way junction. In agreement with this role of eIF3, certain point mutations in the four-way junction allow 48S complex formation with normal eIF2 and eIF3 in in vitro translation systems while preventing subunit association (Ji et al., 2004).

In conclusion, the HCV IRES domains act synergistically to position the initiation codon in the ribosomal P site. In a simplistic model, the HCV IRES could act like a lever, with the pseudoknot and the four-way junction as two lever arms (Figure 7C). Domain 3d could be envisaged as the pivot point of a lever movement that is necessary for the proper positioning of the initiation codon and subunit joining. We suggest tentatively that this movement may be induced by binding of eIF3 to the four-way junction.

Comparison of Translation Initiation of HCV and CrPV IRES

The structure of the HCV IRES-80S complex may be compared to structures of the CrPV IRES-80S complex which facilitate the initiation of translation in the absence of canonical initiation factors (Spahn et al., 2004). The CrPV IRES-80S complex was stalled before the first translocation step (Pestova and Hellen, 2003) by omission of elongation factors. The position of the IRES in the HCV and the CrPV IRES-80S complexes is different. Whereas the HCV IRES is largely located on the solvent side of the 40S subunit, with the exception of domain 2, the CrPV IRES is located entirely in the mRNA binding cleft, reaching into the P and A sites. The different modes of IRES binding probably reflect the different modes of initiation codon binding. In the case of CrPV, the initiation codon is positioned by internal base pairing of the CrPV IRES. In contrast, the HCV IRES probably requires the interactions on the solvent side of the 40S subunit to facilitate a stable binding of the initiation codon that is recognized by tRNA$_i^{MET}$ in the ternary complex.

Contacts shared by the two IRES elements occur on protein S5 on the 40S subunit and on the L1 stalk on the 60S subunit. These may be required for subunit joining and progression to elongation. Both structures alter the conformation of the 80S ribosome significantly compared to the vacant 80S ribosome (Spahn et al., 2004). In both structures, helix 16 is in contact with protein S3 of the head. However, the conformation of the mRNA entry channel differs between these two structures. Whereas in the HCV IRES-80S complex the mRNA entry channel is closed by an interaction between helices 34 and 18, in the case of the CrPV IRES-80S structure, the channel is open. In the HCV IRES-80S structure, the closure of the mRNA entry channel is accompanied by a conformational change of the head beak; this change is absent in CrPV IRES-80S. Thus, as suggested above, the stable binding of the initiation codon in the 48S complex may be accompanied by conformational changes of the mRNA entry channel. These changes may be absent in the case of pseudoelongation of CrPV IRES which does not require a ternary complex (Met-tRNA$_i^{MET}$/eIF2/GTP). In conclusion, the location of different IRES elements seems to vary according to the mode of positioning of the initiation codon, but they still share the remarkable ability to alter actively the ribosome conformation to a "translation initiation competent" state. This activity may allow the IRES elements to initiate translation under conditions of translational repression, when the host cell's defense prohibits the action of translational initiation factors.

Experimental Procedures

HCV IRES mRNA Preparation

The tobramycin aptamer-tagged HCV IRES mRNA (Tob-IRES mRNA nt 1–372) and untagged IRES RNA (IRES) used in this study were prepared by transcription and were purified as described previously (Ostareck-Lederer et al., 2005).

Preparation of the Tobramycin Affinity Matrix

N-hydroxysuccinimide-activated Sepharose 4 Fast Flow was modified with 5 mM tobramycin as described elsewhere (Wang and Rando, 1995). All further procedures were performed at 4ºC unless otherwise stated. For purification of the 80S complex, 70 μl of the tobramycin matrix was blocked with 1 ml of blocking buffer (20 mM Tris.HCl [pH 8.1], 300 mM KCl, 1 mM CaCl$_2$, 5 mM MgCl$_2$, 0.2 mM DTT, 0.1 mg/ml tRNA, 0.5 mg/ml BSA, 0.01% Nonidet P-40) before pooled gradient fractions were added.

Translation Initiation Reaction and 80S Complex Purification

Translation initiation intermediates binding to radiolabeled HCV IRES mRNA and Tob-HCV IRES mRNA were assembled in a 1.5 ml translation initiation reaction containing HeLa cell extract (40%), 100 μM amino acid mix, 16 mM HEPES (pH 7.6), 4.5 mM Mg(OAc)$_2$, 125 mM KOAc, 8 μg/ml calf liver tRNA (final concentration 8 ng/μl), 0.8 mM ATP, 0.1 mM GTP, 20 mM creatine phosphate, 40 μg/ml creatine kinase (final concentration 40 μg/ml), and 1 mM cycloheximide. The reaction mixture was preincubated for 3 min at 30ºC and then 312 pmol Tob-tagged HCV IRES mRNA was added. The mixture was incubated for 5 min at 30ºC. Initiation complexes were resolved on a 5%–25% linear sucrose gradient using the tobramycin binding buffer as gradient buffer (20 mM Tris.HCl [pH 8.1], 145 mM KCl, 1 mM CaCl$_2$, 5 mM MgCl$_2$, 0.2 mM DTT). Sucrose fractions (250 μl each) were collected from the bottom of the gradient and were analyzed by scintillation counting. The fractions containing the 80S translation complex were pooled and 1.25 ml of the pooled fractions was incubated with 70 μl preblocked tobramycin beads for 1 hr at 4ºC with constant head-over-tail rotation. The matrix was washed three times with 1 ml wash buffer (20 mM Tris.HCl [pH 8.1], 145 mM KCl, 1 mM CaCl$_2$, 5 mM MgCl$_2$, 0.2 mM DTT, 0.01% NP-40). Complexes were eluted by incubating with 150 μl of elution buffer (gradient buffer containing 5 mM tobramycin) for 20 min at 4ºC with constant head-over-tail rotation. For the isolation of elongating ribosomes on cellular mRNA, HeLa cell extract was incubated with 1 mM cycloheximide and loaded onto a 5%–25% sucrose gradient in tobramycin binding buffer. Fractions of 250 μl were collected and analyzed by UV spectrometry. The 80S peak fraction was used for electron microscopic studies. Silver staining was performed according to the manufacturer's protocol (protein silver staining kit, Amersham Biosciences, Little Chalfont, UK).

Electron Microscopy

A solution of IRES-80S complex or cycloheximide-treated 80S ribosomes was applied to a perforated carbon foil on a grid and vitrified by plunging into liquid ethane (Dubochet et al., 1988). The grids were kept at liquid nitrogen temperature and imaged in a Philips CM200 FEG microscope (Philips Electron Optics, Eindhoven, The Netherlands) at an acceleration voltage of 200 kV under low-dose conditions at 2–4 μm defocus on Kodak SO-163 film (Eastman Kodak, Rochester, NY). For the IRES-80S complex, the magnification was 50,000×. The images were scanned with a rotating drum scanner (Heidelberger Druckmaschinen, Heidelberg, Germany) at a step size of 4 μm, and computationally coarsened to a final pixel size of 3.6 Å. A total of 24,100 single-particle images were used for image processing. For the elongating 80S ribosomes, the magnification was 38,000×. The images were scanned with the same rotating drum scanner at a step size of 10 μm and computationally coarsened to a final pixel size of 5.57 Å. A total of 10,900 single-particle molecular images were used for image processing.

Image Processing

Imagic-5 software was used. Briefly, after a "reference-free" alignment procedure (alignment by classification; Dube et al., 1993), images were subjected to a multivariate statistical analysis (van Heel and Frank, 1981) and classification. The class averages were used

for 3D structure determination by the angular reconstitution approach (van Heel, 1987). The 3D structure of the 80S rabbit ribosome (Dube et al., 1998) was used for the first angle assignment. The structure was refined as described elsewhere (van Heel et al., 1996). The resolution of the structures was calculated by the Fourier shell correlation function using the 3 σ criterion and the 0.5 criterion: for the IRES-80S complex, the resolution was found to be, respectively, 15 Å and 25 Å, and for the cycloheximide-treated 80S ribosome, it was 28 Å and 35 Å (see Supplemental Data). All fitting was done manually by using the visualization software Amira (TGS Europe, Merignac Cedex, France). The RNA and protein components of the 40S subunit of the IRES-80S complex were assigned by fitting the atomic homology model of the yeast ribosome Protein Data Bank code 1K5X (Spahn et al., 2001a). The HCV IRES density was fitted by using RNA structures deposited in the PDB database: these were codes 1P5P, 1F84, 1KH6, and 1KP7 for the HCV IRES domains 2, 3d, and four-way junction including 3a/c and domain 3b.

Supplemental Data

Supplemental data, including three figures, can be found with this article online at http://www.structure.org/cgi/content/full/13/11/1695/DC1/.

References

Beales, L.P., Rowlands, D.J., and Holzenburg, A. (2001). The internal ribosome entry site (IRES) of hepatitis C virus visualized by electron microscopy. RNA 7, 661–670.

Beckmann, R., Spahn, C.M., Eswar, N., Helmers, J., Penczek, P.A., Sali, A., Frank, J., and Blobel, G. (2001). Architecture of the protein-conducting channel associated with the translating 80S ribosome. Cell 107, 361–372.

Bergamini, G., Preiss, T., and Hentze, M.W. (2000). Picornavirus IRESes and the poly(A) tail jointly promote cap-independent translation in a mammalian cell-free system. RNA 6, 1781–1790.

Brown, E.A., Zhang, H., Ping, L.H., and Lemon, S.M. (1992). Secondary structure of the 5′ nontranslated regions of hepatitis C virus and pestivirus genomic RNAs. Nucleic Acids Res. 20, 5041–5045.

Buratti, E., Tisminetzky, S., Zotti, M., and Baralle, F.E. (1998). Functional analysis of the interaction between HCV 5′UTR and putative subunits of eukaryotic translation initiation factor eIF3. Nucleic Acids Res. 26, 3179–3187.

Collier, A.J., Gallego, J., Klinck, R., Cole, P.T., Harris, S.J., Harrison, G.P., Aboul-Ela, F., Varani, G., and Walker, S. (2002). A conserved RNA structure within the HCV IRES eIF3-binding site. Nat. Struct. Biol. 9, 375–380.

Dmitriev, S.E., Pisarev, A.V., Rubtsova, M.P., Dunaevsky, Y.E., and Shatsky, I.N. (2003). Conversion of 48S translation preinitiation complexes into 80S initiation complexes as revealed by toeprinting. FEBS Lett. 533, 99–104.

Dube, P., Tavares, P., Lurz, R., and van Heel, M. (1993). The portal protein of bacteriophage SPP1: a DNA pump with 13-fold symmetry. EMBO J. 12, 1303–1309.

Dube, P., Bacher, G., Stark, H., Mueller, F., Zemlin, F., van Heel, M., and Brimacombe, R. (1998). Correlation of the expansion segments in mammalian rRNA with the fine structure of the 80 S ribosome; a cryoelectron microscopic reconstruction of the rabbit reticulocyte ribosome at 21 Å resolution. J. Mol. Biol. 279, 403–421.

Dubochet, J., Adrian, M., Chang, J.J., Homo, J.C., Lepault, J., McDowall, A.W., and Schultz, P. (1988). Cryo-electron microscopy of vitrified specimens. Q. Rev. Biophys. 21, 129–228.

Fukushi, S., Okada, M., Stahl, J., Kageyama, T., Hoshino, F.B., and Katayama, K. (2001). Ribosomal protein S5 interacts with the internal ribosomal entry site of hepatitis C virus. J. Biol. Chem. 276, 20824–20826.

Hamasaki, K., Killian, J., Cho, J., and Rando, R.R. (1998). Minimal RNA constructs that specifically bind aminoglycoside antibiotics with high affinities. Biochemistry 37, 656–663.

Hartmuth, K., Urlaub, H., Vornlocher, H.P., Will, C.L., Gentzel, M., Wilm, M., and Lührmann, R. (2002). Protein composition of human prespliceosomes isolated by a tobramycin affinity-selection method. Proc. Natl. Acad. Sci. USA 99, 16719–16724.

Hershey, J.W.B., and Merrick, W.C. (2000). The pathway and mechanism of initiation of protein synthesis. In Translational Control of Gene Expression, J.W.B. Hershey and M.B. Mathews, eds. (Cold Spring Harbor, NY: Cold Spring Harbor Laboratory Press), pp. 33–88.

Honda, M., Brown, E.A., and Lemon, S.M. (1996). Stability of a stem-loop involving the initiator AUG controls the efficiency of internal initiation of translation on hepatitis C virus RNA. RNA 2, 955–968.

Ji, H., Fraser, C.S., Yu, Y., Leary, J., and Doudna, J.A. (2004). Coordinated assembly of human translation initiation complexes by the hepatitis C virus internal ribosome entry site RNA. Proc. Natl. Acad. Sci. USA 101, 16990–16995.

Jubin, R., Vantuno, N.E., Kieft, J.S., Murray, M.G., Doudna, J.A., Lau, J.Y., and Baroudy, B.M. (2000). Hepatitis C virus internal ribosome entry site (IRES) stem loop IIId contains a phylogenetically conserved GGG triplet essential for translation and IRES folding. J. Virol. 74, 10430–10437.

Kieft, J.S., Zhou, K., Jubin, R., and Doudna, J.A. (2001). Mechanism of ribosome recruitment by hepatitis C IRES RNA. RNA 7, 194–206.

Kieft, J.S., Zhou, K., Grech, A., Jubin, R., and Doudna, J.A. (2002). Crystal structure of an RNA tertiary domain essential to HCV IRES-mediated translation initiation. Nat. Struct. Biol. 9, 370–374.

Klinck, R., Westhof, E., Walker, S., Afshar, M., Collier, A., and Aboul-Ela, F. (2000). A potential RNA drug target in the hepatitis C virus internal ribosomal entry site. RNA 6, 1423–1431.

Kolupaeva, V.G., Pestova, T.V., and Hellen, C.U. (2000). An enzymatic footprinting analysis of the interaction of 40S ribosomal subunits with the internal ribosomal entry site of hepatitis C virus. J. Virol. 74, 6242–6250.

Lilley, D.M. (2000). Structures of helical junctions in nucleic acids. Q. Rev. Biophys. 33, 109–159.

Lukavsky, P.J., Otto, G.A., Lancaster, A.M., Sarnow, P., and Puglisi, J.D. (2000). Structures of two RNA domains essential for hepatitis C virus internal ribosome entry site function. Nat. Struct. Biol. 7, 1105–1110.

Lukavsky, P.J., Kim, I., Otto, G.A., and Puglisi, J.D. (2003). Structure of HCV IRES domain II determined by NMR. Nat. Struct. Biol. 10, 1033–1038.

Lyons, A.J., Lytle, J.R., Gomez, J., and Robertson, H.D. (2001). Hepatitis C virus internal ribosome entry site RNA contains a tertiary structural element in a functional domain of stem-loop II. Nucleic Acids Res. 29, 2535–2541.

Lytle, J.R., Wu, L., and Robertson, H.D. (2001). The ribosome binding site of hepatitis C virus mRNA. J. Virol. 75, 7629–7636.

Melcher, S.E., Wilson, T.J., and Lilley, D.M. (2003). The dynamic nature of the four-way junction of the hepatitis C virus IRES. RNA 9, 809–820.

Menetret, J.F., Neuhof, A., Morgan, D.G., Plath, K., Radermacher, M., Rapoport, T.A., and Akey, C.W. (2000). The structure of ribosome-channel complexes engaged in protein translocation. Mol. Cell 6, 1219–1232.

Morgan, D.G., Menetret, J.F., Neuhof, A., Rapoport, T.A., and Akey, C.W. (2002). Structure of the mammalian ribosome-channel complex at 17Å resolution. J. Mol. Biol. 324, 871–886.

Nilsson, J., Sengupta, J., Frank, J., and Nissen, P. (2004). Regulation of eukaryotic translation by the RACK1 protein: a platform for signalling molecules on the ribosome. EMBO Rep. *5*, 1137–1141.

Odreman-Macchioli, F., Baralle, F.E., and Buratti, E. (2001). Mutational analysis of the different bulge regions of hepatitis C virus domain II and their influence on internal ribosome entry site translational ability. J. Biol. Chem. *276*, 41648–41655.

Ostareck-Lederer, A., Clauder-Münster, S., Therman, R., Polycarpou-Schwarz, M., Gentzel, M., Wilm, M., and Lewis, J.D. (2005). The role of RNA interference in drug target validation: application to hepatitis C. In RNA Interference Technology: From Basic Science to Drug Development, K. Appasani, ed. (Cambridge, UK: Cambridge University Press), pp. 318–331.

Otto, G.A., and Puglisi, J.D. (2004). The pathway of HCV IRES-mediated translation initiation. Cell *119*, 369–380.

Pestova, T.V., and Hellen, C.U. (2003). Translation elongation after assembly of ribosomes on the Cricket paralysis virus internal ribosomal entry site without initiation factors or initiator tRNA. Genes Dev. *17*, 181–186.

Pestova, T.V., Shatsky, I.N., Fletcher, S.P., Jackson, R.J., and Hellen, C.U. (1998). A prokaryotic-like mode of cytoplasmic eukaryotic ribosome binding to the initiation codon during internal translation initiation of hepatitis C and classical swine fever virus RNAs. Genes Dev. *12*, 67–83.

Pestova, T.V., Kolupaeva, V.G., Lomakin, I.B., Pilipenko, E.V., Shatsky, I.N., Agol, V.I., and Hellen, C.U. (2001). Molecular mechanisms of translation initiation in eukaryotes. Proc. Natl. Acad. Sci. USA *98*, 7029–7036.

Reynolds, J.E., Kaminski, A., Carroll, A.R., Clarke, B.E., Rowlands, D.J., and Jackson, R.J. (1996). Internal initiation of translation of hepatitis C virus RNA: the ribosome entry site is at the authentic initiation codon. RNA *2*, 867–878.

Rijnbrand, R., Thiviyanathan, V., Kaluarachchi, K., Lemon, S.M., and Gorenstein, D.G. (2004). Mutational and structural analysis of stem-loop IIIC of the hepatitis C virus and GB virus B internal ribosome entry sites. J. Mol. Biol. *343*, 805–817.

Scheper, G.C., and Proud, C.G. (2002). Does phosphorylation of the cap-binding protein eIF4E play a role in translation initiation? Eur. J. Biochem. *269*, 5350–5359.

Sengupta, J., Nilsson, J., Gursky, R., Spahn, C.M., Nissen, P., and Frank, J. (2004). Identification of the versatile scaffold protein RACK1 on the eukaryotic ribosome by cryo-EM. Nat. Struct. Mol. Biol. *11*, 957–962.

Sizova, D.V., Kolupaeva, V.G., Pestova, T.V., Shatsky, I.N., and Hellen, C.U. (1998). Specific interaction of eukaryotic translation initiation factor 3 with the 5′ nontranslated regions of hepatitis C virus and classical swine fever virus RNAs. J. Virol. *72*, 4775–4782.

Spahn, C.M., Beckmann, R., Eswar, N., Penczek, P.A., Sali, A., Blobel, G., and Frank, J. (2001a). Structure of the 80S ribosome from *Saccharomyces cerevisiae*—tRNA-ribosome and subunit-subunit interactions. Cell *107*, 373–386.

Spahn, C.M., Kieft, J.S., Grassucci, R.A., Penczek, P.A., Zhou, K., Doudna, J.A., and Frank, J. (2001b). Hepatitis C virus IRES RNA-induced changes in the conformation of the 40S ribosomal subunit. Science *291*, 1959–1962.

Spahn, C.M., Jan, E., Mulder, A., Grassucci, R.A., Sarnow, P., and Frank, J. (2004). Cryo-EM visualization of a viral internal ribosome entry site bound to human ribosomes: the IRES functions as an RNA-based translation factor. Cell *118*, 465–475.

Tsukiyama-Kohara, K., Iizuka, N., Kohara, M., and Nomoto, A. (1992). Internal ribosome entry site within hepatitis C virus RNA. J. Virol. *66*, 1476–1483.

Valle, M., Zavialov, A., Sengupta, J., Rawat, U., Ehrenberg, M., and Frank, J. (2003). Locking and unlocking of ribosomal motions. Cell *114*, 123–134.

van Heel, M. (1987). Angular reconstitution: a posteriori assignment of projection directions for 3D reconstruction. Ultramicroscopy *21*, 111–123.

van Heel, M., and Frank, J. (1981). Use of multivariate statistics in analysing the images of biological macromolecules. Ultramicroscopy *6*, 187–194.

van Heel, M., Harauz, G., Orlova, E.V., Schmidt, R., and Schatz, M. (1996). A new generation of the IMAGIC image processing system. J. Struct. Biol. *116*, 17–24.

Wang, Y., and Rando, R.R. (1995). Specific binding of aminoglycoside antibiotics to RNA. Chem. Biol. *2*, 281–290.

Wang, C., Sarnow, P., and Siddiqui, A. (1993). Translation of human hepatitis C virus RNA in cultured cells is mediated by an internal ribosome-binding mechanism. J. Virol. *67*, 3338–3344.

Wang, C., Le, S.Y., Ali, N., and Siddiqui, A. (1995). An RNA pseudoknot is an essential structural element of the internal ribosome entry site located within the hepatitis C virus 5′ noncoding region. RNA *1*, 526–537.

Yusupova, G.Z., Yusupov, M.M., Cate, J.H., and Noller, H.F. (2001). The path of messenger RNA through the ribosome. Cell *106*, 233–241.

Zhao, W.D., and Wimmer, E. (2001). Genetic analysis of a poliovirus/hepatitis C virus chimera: new structure for domain II of the internal ribosomal entry site of hepatitis C virus. J. Virol. *75*, 3719–3730.

Accession Numbers

Structural coordinates have been deposited in the Protein Data Bank (code 2AGN) and in the IIMS Database at EMBL EBI (code EMD-1138).